Received: 20 July 2023 | Revised: 24 August 2023 | Accepted: 29 August 2023 | Published online: 31 August 2023

RESEARCH ARTICLE

Archives of Advanced Engineering Science
2025, Vol. 3(2) 73–82
DOI: 10.47852/bonviewAAES32021384

BON VIEW PUBLISHING

Feasibility Study of Theoretical Efficiency Calculation for Flat-Plate Collectors in Solar Water Heating Systems

Sayed Ahmad Zamir Fatemi[1,*], Wahidullah Zgham[1], Safiullah Shirzad[1] and Zainullah Serat[1]

[1]*Energy Engineering Department, Ghazni Technical University, Afghanistan*

Abstract: Solar energy stands as a paramount clean, abundant, and renewable power source holding remarkable potential to address our escalating energy needs. Among its crucial utilization methods, solar water heating systems integrating flat-plate collectors (FPCs) emerge as vital contributors in harnessing and converting solar energy into utilizable heat. This study delves into the realm of FPCs' theoretical efficiency assessment, employing mathematical models and factoring regional weather conditions to meticulously evaluate the efficiency of single-glazed and double-glazed collector variants. The outcomes spotlight the single-glazed collector's efficiency at 0.669 and the double-glazed collector at 0.713, underscoring the discernible performance gap. In a landscape where industries, hospitals, residences in Kandahar, and comparable settings extensively depend on hot water, often derived from fossil fuel-driven heating, this research's implications hold particular relevance. By transitioning toward solar water heating, this study underscores a concrete method not only to curtail carbon emissions but also to significantly reduce energy expenses linked with conventional heating techniques. The findings beckon a departure from the status quo, emphasizing that cleaner energy options are attainable, even for regions demanding hot water requirements. As society navigates complex decisions concerning energy sourcing, embracing solar water heating stands as an auspicious stride toward a sustainable future, beckoning us to collectively embark on a path of energy-conscious choices for the greater good of our planet and the generations that will inhabit it.

Keywords: theoretical efficiency, flat-plate collector, solar water heating system

1. Introduction

Bringing new technology to use free and green energy for a poor nation is a benefit, this article compares and evaluates the effectiveness, reliability, and efficiency of flat-plate solar collectors used in solar water heating systems to supply hot water for home and industrial usage. The efficiency is defined as the ratio of the sound energy delivered to the energy incident on the collector aperture [1]. Energy is necessary for a country and society's essential development, and energy and electricity play a crucial role in the economy's growth. Renewable energy sources have the potential to reduce greenhouse gas emissions such as carbon dioxide [2]. Solar energy is one of the main forms of renewable energy and may be utilized to produce both electrical and thermal energy. Heat energy is usually generated using three distinct types of solar collectors: evacuated tube collectors, flat-plate collectors (FPCs), and parabolic trough collectors. Each type of collector is designed for specific applications [3]. Evacuated tube collectors find application in domestic water heating systems where pressurized water is not required. The FPC is used for both domestic and industrial purposes, where pressurized water is needed. On the other hand, concentrating collectors or parabolic trough collectors are employed solely in industrial applications due to their pressurized output water with high-temperature requirement [1]. The collector's types according to their working temperature and usage are summarized in Table 1 [4].

The FPC is suitable for both domestic and industrial applications, depending on the desired output of the collector [5]. What is the performance and efficiency of flat-plate solar collectors in domestic water heating? How can the technology be optimized to increase cost-effectiveness and reduce reliance on non-renewable energy sources? Even though Afghanistan is one of the most backward nations, there are plenty of energy resources available such as biomass, hydroelectric, and coal mines; however, they cannot provide the energy needs of all Afghans, Therefore, it is vital to use a different kind of energy that is clean, endless, and environmentally safe, although solar photovoltaic modules are used more frequently every day in the nation as an electric energy source; however, not all of the families' requirements can be satisfied. We aim to utilize the sun's energy in different ways, such as heating water with the use of solar collectors, to close the energy gap in the nation [6, 7]. Solar water heaters offer a range of advantages, such as cost-effective energy, minimal noise emissions, eco-friendly power source, and their role in promoting sustainable and environmentally conscious water heating systems [8]. Fluid tube solar collectors, also known as Flat Plate Collectors (FPCs), consist of tubes filled with a flowing heat transfer fluid (HTF) connected to a black surface with high absorptivity. This surface can collect direct and diffuse solar radiation and transfer the

***Corresponding author:** Sayed Ahmad Zamir Fatemi, Energy Engineering Department, Ghazni Technical University, Afghanistan. Email: sayedAZF@teug.edu.af; fatemi.zamir@gmail.com

Table 1
Types of solar collectors and their corresponding working temperatures

Solar collector type	Working temperature range	Application
Flat plate collector (FPC)	40 °C–80 °C	Domestic and industrial water heating
Evacuated tube collector	70 °C–120 °C	Domestic water heating, space heating
Parabolic trough collector	150 °C–400 °C	Industrial processes, Power generation

heat to the tubes. The absorber is protected by a transparent cover to reduce both convection and radiation heat losses. An efficient thermal insulation casing is also used to limit conduction losses [9, 10]. This technology is suitable for low-temperature applications such as hot water, and it can achieve reasonable thermal efficiencies because heat losses are minimal. A schematic view of FPC is shown in Figure 1 [1].

Figure 1
Schematic view of a FPC

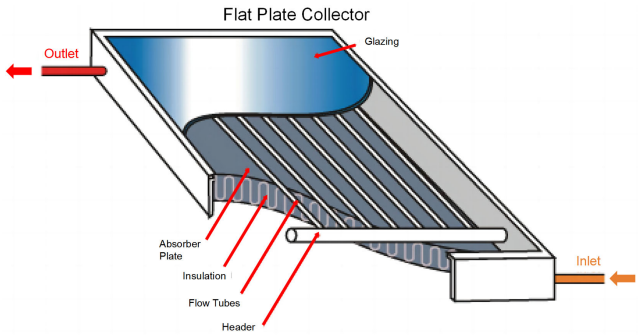

When the sun's rays penetrate the transparent cover and reach a blackboard with high absorptivity, a significant portion of this energy is absorbed by the surface, converted into heat, and then transferred to liquid-filled tubes; these tubes transport the heat to a storage tank or a storage space [11]. In order to minimize conductivity losses, a reflective material is applied to the lower portion and both sides of the absorber plate. Additionally, the liquid tubes are securely attached to the absorber plate and have the capability to cover the entire surface [12, 13]. The small tubes are connected to larger tubes called headers, and the tube that carries the heated liquid upwards is called the riser, the header and riser of the collector have a specialized design to maximize the absorption of solar energy [14]. The key elements of a FPC, shown in Figure 2 [1]:

1) A cover made of one or multiple sheets of radiation-transmitting material, such as glass.
2) Heat removal fluid passageways, such as tubes, fins, or passages, facilitate the flow of HTF from the inlet to the outlet.

Figure 2
Exploded view of a flat-plate collector and absorber details

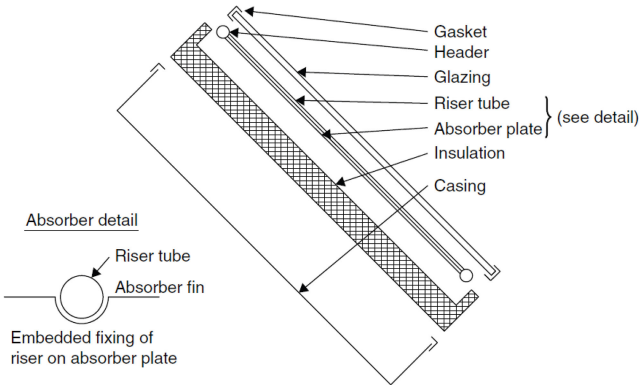

3) An absorber plate that is typically flat, corrugated, or grooved, and to which the tubes, fins, or passages are attached.
4) Headers or manifolds are pipes and ducts used to introduce and discharge the fluid.
5) Insulation helps to minimize heat loss from the back and sides of the collector.
6) A container that surrounds and safeguards the aforementioned components from environmental factors like dust, moisture, and other materials.

Solar collectors are often glazed with glass due to its ability to transmit up to 90% of shortwave solar irradiation while blocking nearly all of the longwave radiation emitted outward by the absorber plate, this is why the glass has been extensively used as a glazing material for solar collectors [15]. Ordinary window glass is typically unsuitable for solar collectors due to its high iron content. However, glass with low iron content has a relatively high transmittance for solar radiation, typically around 0.85–0.90 when the radiation hits it directly. Nonetheless, this same glass has almost zero transmittance for the longwave thermal radiation (5.0–50 μm) emitted by sun-heated surfaces [1]. Plastic films and sheets also have high shortwave transmittance, which means they can let in a significant amount of solar radiation. However, most usable types of plastics also have transmission bands in the middle of the thermal radiation spectrum, leading to longwave transmittances that can be as high as 0.40; moreover, plastics have limited heat tolerance and may deteriorate or undergo dimensional changes when exposed to high temperatures. Only a few types of plastics can withstand the sun's ultraviolet radiation for extended periods; however, plastic films are resistant to damage from hail or stones, and they are flexible and lightweight when in thin form [16].

Polvongsri and Kiatsiriroat [17] investigated the performance of solar water collectors using silver nanofluid. The experiment involved three small flat-plate solar collectors (0.15 m × 1.0 m) with 1000 and 10,000 ppm silver concentrations. Varying the mass flux (0.8–1.2 L/min-m^2) and controlling inlet temperatures (35 °C–65 °C), the study found that the nanofluid exhibited higher heat transfer coefficients than water, particularly at 10,000 ppm. This reduced heat loss and increased solar heat gain, especially at high inlet temperatures. Optical and thermal loss characteristics indicated that silver nanoparticles contributed to lower thermal losses in the collector, highlighting the potential of

silver nanofluids for enhancing solar water collector performance and promoting efficient, sustainable solar energy utilization.

This study addresses the challenge of assessing the performance of flat-plate solar collectors in southern Afghanistan, with a specific focus on Kandahar and other regions experiencing similar climate conditions. The outcomes of this study are intended to assist designers and users in evaluating their initial designs and estimating the required solar absorber area for water heating systems. By doing so, the goal is to promote the adoption of solar energy systems, thereby diminishing reliance on fossil fuels and mitigating environmental issues. Furthermore, this endeavor aims to contribute to the global concern of climate change by supporting the sustainable and economical utilization of renewable energy sources within this geographical area.

2. Research Methodology

2.1. Site selection

The selection of Kandahar, Afghanistan, which is located between 65.6975° longitude in the east and 31.6371° of latitude in the north, 1010 m high above sea level with the ground reflectance or albedo 0.2, as the focal point of this study stems from several crucial factors [18]. Firstly, Kandahar and its surrounding areas suffer from a lack of reliable electricity supply, particularly in remote residential areas and industrial zones, this implements alternative energy sources, such as solar water heaters, highly desirable to meet the growing demand for hot water. Secondly, the prevalent use of wood, coal, and fossil fuels for heating purposes in both industrial and residential sectors has resulted in severe environmental impacts, including air pollution, and carbon emissions. By examining the system efficiency of solar water heaters in Kandahar, this research aims to highlight the potential environmental benefits and cost-effectiveness of adopting solar energy solutions as alternatives to traditional fuel sources [19]. The findings of this study can contribute to the formulation of sustainable energy policies and strategies for Kandahar and other regions facing similar energy and environmental challenges. Figure 3 shows a map of Kandahar province.

Figure 3
Map of Kandahar Province

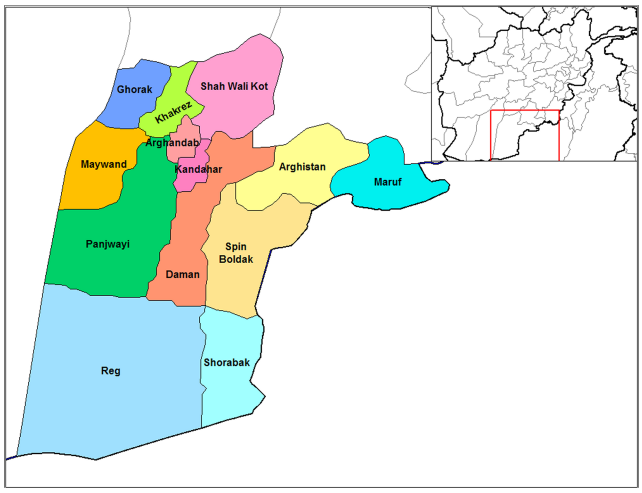

2.2. Solar collector selection

Solar energy collectors that convert sunlight into useful heat come in various types, with the most popular ones being the evacuated tube collector, FPC, and parabolic trough collector [20]. Among these, the FPC proves suitable for both domestic and industrial applications, determined by its output capacity, ease of construction, installation, and maintenance procedures. These collectors exist in multiple variants, with differing glazing options including single glazing and double glazing, each impacting factors such as heat loss and radiation transmittance. In the context of this study, the chosen collector type is the FPC, encompassing both single and double glazing, and this configuration will be the subject of evaluation.

2.3. Weather condition

2.3.1. Temperature

In the selected area, which is 1010 m above sea level, the winters are chilly, dry, and typically clear, while the summers are lengthy, hot, arid, and clear. The temperature rarely falls below −2.7 °C or rises over 42.7 °C throughout the year, often fluctuating between 1.1 °C and 40 °C [21]. Kandahar, Afghanistan, typically experiences around 300 sunny days per year, with an average of 5.96 peak hours of sunlight per day throughout the years [22]. This abundance of sunshine makes Kandahar an excellent location for harnessing solar energy through the use of solar collectors. Additionally, the hot weather prevalent in Kandahar further enhances the region's potential for solar energy utilization. Figure 4 [21] shows the high and low temperatures every month during the year.

Figure 4
The monthly average high and low temperature

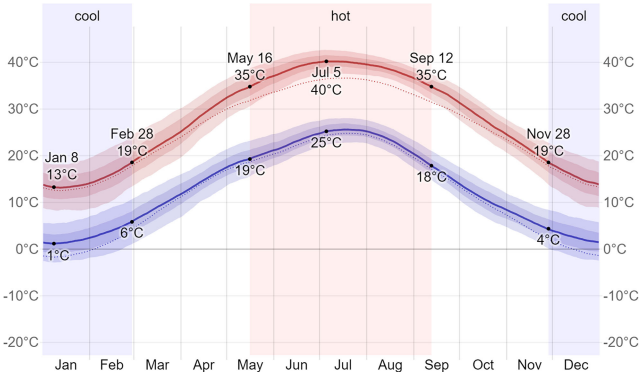

2.3.2. Solar insolation

Solar insolation refers to the amount of solar radiation received on a given surface area over a specific period [14]. Kandahar, Afghanistan, is characterized by high solar insolation, making it an ideal location for harnessing solar energy [22]. Situated in a region with a predominantly arid and sunny climate, Kandahar receives abundant sunlight throughout the year, with an average annual solar radiation ranging from 5 to 6 kWh/m^2 per day [21]. This ample solar resource provides a promising foundation for the

Figure 5
Sun path diagram for Kandahar

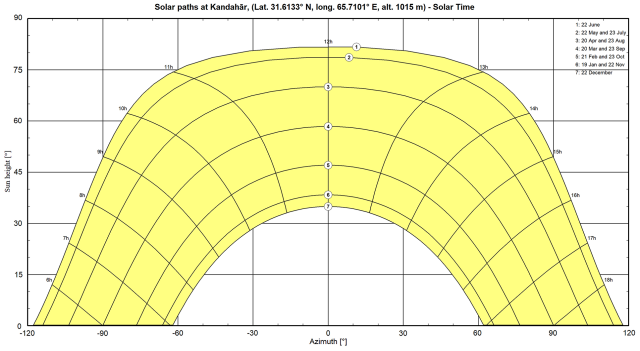

Figure 6
Average wind speed in Kandahar

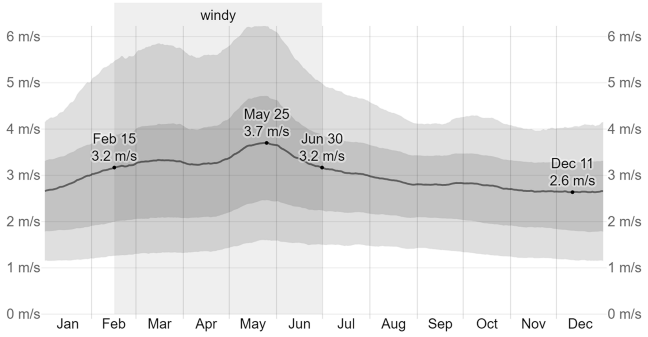

efficient operation of solar water heating systems. Quantifying and analyzing the solar insolation levels in Kandahar, to establish a comprehensive understanding of the solar energy potential in the region, will serve as a valuable basis for evaluating and optimizing the system efficiency of solar water heaters in this specific context.

Figure 5 [18] shows that during the summer solstice, which occurs around the 22nd of June, the sun follows a high path in the sky. The solar azimuth angle reaches its minimum at 5:00 AM, with a value of −120°, indicating a more northern position. As the day progresses, the sun's azimuth angle gradually increases, reaching its maximum of +120° at 07:00 PM. At absolute noon, when the sun is at its highest point in the sky, the solar azimuth angle is 0°, and the sun's height reaches its maximum of 80°. On the other hand, during the winter solstice, around 22nd of December, the sun takes a lower path in the sky. At 07:12 AM, the solar azimuth angle is −62°, indicating a more southern position in the sky. By 05:48 PM, the solar azimuth angle reaches its maximum value of +62°, as the sun moves toward the northern part of the sky. At absolute noon, the solar azimuth angle is again 0°, but the sun's height is reduced to 34° compared to the summer solstice. By studying the sun path diagram, we can gain insights into the changing position of the sun throughout the year, which has implications for daylight availability, shading, and solar energy capture in Kandahar, Afghanistan, located in the Northern Hemisphere.

2.3.3. Wind speed

The wind period in Kandahar is approximately 4.5 months, starting from February 15 and ending on July 1, during which the average wind speeds exceed 3.1 m/s. Among these months, May is the windiest, with an average hourly wind speed of 3.62 m/s. On the other hand, the calmer season lasts for around 7.5 months, extending from July 1 to February 15. December is the calmest month in Kandahar, with an average hourly wind speed of 2.64 m/s. The prevailing wind direction in Kandahar changes throughout the year. For 10 months, from January 25 to November 26, the wind predominantly blows from the west, reaching a peak frequency of 59% on May 18. During the remaining 2.0 months, from November 26 to January 25, the wind predominantly originates from the east, with a peak frequency of 38% in January 1 [21]. Figure 6 [21] shows the average wind speed for Kandahar.

2.4. Data collection

The specifications of the selected solar collector can be found in Table 2. This table provides detailed information on the collector's characteristics, such as its dimensions, materials used, and efficiency ratings. These specifications play a crucial role in determining the performance and effectiveness of the solar collector in harnessing solar energy.

Table 3 [23] presents climatic data tailored to the research area of Kandahar city, Afghanistan. The data encompass key variables including global horizontal radiation (Global H), diffuse horizontal radiation (Diffuse H), temperature, and wind velocity. These measurements are documented for each month throughout the year, facilitating a thorough examination of the annual fluctuations in these parameters. Furthermore, the table outlines

Table 2
Flat-plate collector's specifications

Name	Qty
Area (sqm)	2
Length (m)	2
Width (m)	1
No. of glass	1 & 2
Glass thickness (m)	0.004
Glass thermal conductivity (w/m K)	0.5
Glass emissivity	0.88
KL of glass	0.37
Space between absorber plate and glass (m)	0.02
Space between glasses (m)	0.02
Absorber plate thickness (m)	0.0004
Absorber plate material	Copper
Absorber plate thermal conductivity (W/mK)	401
Absorber plate absorptivity	0.9
Absorber plate emissivity	0.1
Back insulation thickness (m)	0.05
Back insulation thermal conductivity (W/mK)	0.05
Edge insulation thickness (m)	0.04
Edge insulation thermal conductivity (W/mK)	0.05
Slope/tilt (degree)	60
Absorber temperature (K)	353
(Ta)	0.88
W Space between tubes (m)	0.12
D Outer diameter of tube (m)	0.015
Di Inter diameter of tube (m)	0.0135

Table 3
Research site solar incident radiation

Month	GlobH MJ/m^2	DiffH MJ/m^2	Temp °C	Wind Vel m/s
January	10.6	4.5	4	2.62
February	11.8	4.9	7.4	2.79
March	22.1	6.3	17.3	2.35
April	23.3	7.7	20.3	2.59
May	29.6	7.8	28.5	2.93
June	29.7	7.4	30.1	2.57
July	29.1	8.9	33.8	2.41
August	27.1	8.2	31	2.17
September	23.8	6.1	26	2.06
October	19.7	5.0	18.9	1.82
November	12.8	4.5	11.8	1.93
December	12.2	4.1	8.8	1.85
Year	251.7	75.4	19.8	2.34

the geographical coordinates, altitude, time zone, and ground reflectance (albedo) characteristics of the location. The table culminates by providing the mean values of global horizontal radiation, diffuse horizontal radiation, temperature, and wind velocity, computed over the entire year.

Global horizontal radiation (Global H) refers to the total solar radiation received on a horizontal surface, considering direct sunlight and diffuse sky radiation. This measurement indicates the total energy available from the sun and is a critical factor in various applications, including solar energy systems and climate studies [24].

Diffuse horizontal radiation (Diffuse H) represents the solar radiation that reaches a surface after scattering due to interactions with molecules and particles in the atmosphere. Unlike direct sunlight, which travels in a straight line, diffuse radiation comes from all directions and contributes to the ambient illumination of an area. These radiation measurements are crucial for understanding the solar energy potential of a location and assessing its climatic conditions. By analyzing the variations in these parameters, researchers can gain insights into the seasonal patterns, energy availability, and atmospheric characteristics of the study area.

Table 4 focuses on the declination and incidence angles. The declination angle, which changes daily, is represented in the table as average values for each month. This angle is vital in determining the tilt and orientation of solar collectors to maximize energy absorption. The incidence angle, calculated for an air mass

Table 4
Monthly average declination and incidence angles

Month	Declination angle on degree	Incidence angle on degree
January	−20.92	0.00
February	−12.95	0.41
March	−2.42	0.75
April	9.41	1.02
May	18.79	1.20
June	23.09	1.28
July	21.18	1.24
August	13.45	1.10
September	2.22	0.86
October	−9.6	0.54
November	−18.91	0.00
December	−23.05	0.00

Table 5
Properties of working fluid (water)

Property	Qty
Density (kg/m^3)	997
Ti C	13
To C	80
h_{fi} W/m^{2}K	84.41437524
mass flow rate (Kg/sec)	0.001
	0.05
Cp (J/KgK)	4180
k (W/mK)	0.6
μ (Pas. sec)	0.001

(AM) of approximately 1.5, is also included in the table, referencing the work of Jalili Jamshidian et al. [25]. This angle provides insights into the optimal positioning of the solar collector for optimal energy capture.

Lastly, Table 5 [26] provides essential properties of the working fluid used in the solar water heating system, with water assumed as the chosen fluid. These properties, such as density and specific heat capacity, are crucial for accurately modeling and predicting the performance of the system. The selection of water as the working fluid is based on its favorable characteristics and widespread availability [26].

2.5. Mathematical modeling

For obtaining the efficiency of flat-palate solar collectors Equation (1) can be used [1].

$$\eta = F_R(\tau) - \frac{U_{L(T_i - T_a)}}{G_t} \tag{1}$$

where F_R is the heat removal factor, $(\tau\alpha)$ is the transitivity absorptivity, U_L is the overall heat loss coefficient, T_i is the fluid inlet temperature, T_a is the ambient temperature, and G_t is the global solar radiation. The equation involves the heat removal factor (F_R), which quantifies the proportion of useful energy gain that would be obtained if the collector-absorbing surface were at the same temperature as the local fluid [1], expressed symbolically:

$$F_R = \frac{Actual\ Outut}{Output\ for\ Palate\ Temperature = Fluid\ inlet\ Temperature} \tag{2}$$

$$\text{Or } F_R = \frac{\dot{m}C_p(T_{f,o} - T_{f,i})}{A_c[S - U_L(T_{f,i} - T_a)]} \tag{3}$$

$$\text{Or } F_R = \frac{\dot{m}C_p}{A_c U_L}\left[1 - \frac{\left(S/U_L\right) - (T_{f,0} - T_a)}{\left(S/U_L\right) - (T_{f,i} - T_a)}\right] \tag{4}$$

$$\text{Or } F_R = \frac{\dot{m}C_p}{A_c U_L}\left[1 - exp\left(-\frac{U_L F' A_c}{\dot{m}C_p}\right)\right] \tag{5}$$

In Equations (3), (4), and (5), $\dot{m}$ is the mass flow rate of fluid entering the collectors, C_p is the specific heat capacity in constant pressure, $T_{f,o}$ is the fluid outlet temperature, $T_{f,i}$ is the fluid inlet temperature, T_a is the ambient temperature, A_c is the collector area, S is the absorbed solar

radiation, U_L is the overall heat loss coefficient, and F' is the collector efficiency factor. For finding F', Equation (6) is used [1].

$$F' = \frac{\frac{1}{U_L}}{\left\{\frac{1}{U_L[D+(W-D)F]} + \frac{1}{C_b} + \frac{1}{\pi D_i h_{fi}}\right\}} \tag{6}$$

In Equation (6), D is the outside diameter of the tube of the collector, D_i is the inside diameter of the tube, W is the space between tubes in the collector, C_b is the bond conductance, and h_{fi} is the heat transfer coefficient inside the tube. For obtaining F, Equation (7) shall be used [1].

$$\mathrm{F} = \frac{\tanh\left[\mathrm{m}(\mathrm{W}-\mathrm{D})/2\right]}{\mathrm{m}(\mathrm{W}-\mathrm{D})} \tag{7}$$

For F, we have to first find m and from Equation (8) we can find it [1].

$$m = \sqrt{\frac{U_L}{K\delta}} \tag{8}$$

In the above Equation (8), K is the thermal conductivity of materials, and δ is the plate thickness.

The h_{fi} can be calculated from Equation (9) and the equation is [26]:

$$h_{fi} = 0.023\ Re^{0.8}\ Pr^{0.4}(k\ /\ D_i) \tag{9}$$

where Re and Pr are the Reynolds and Prandtl numbers, respectively, and k is the thermal conductivity of fluid. The Re and Pr shall be calculated from Equations (10) and (11).

$$Re = \dot{m}D_i\ /\ (A\mu) \tag{10}$$

where $\dot{m}$ is the mass flow rate of water, A is the cross-sectional area of the tube, and μ is the kinematic viscosity of water.

$$Pr = \mu\ C_p\ /\ k \tag{11}$$

Here, μ is the kinematic viscosity of water, C_{p} is the specific heat at constant pressure, and k is the thermal conductivity of water.

In the above Equations (3)–(5), we have U_L(overall heat loss coefficient), which is the sum of three other heat loss coefficients such as U_t top heat loss coefficient, U_b bottom loss coefficient, and U_e edge heat loss coefficient, which is given by Equation (12) below [1].

$$U_L = U_t + U_b + U_e \tag{12}$$

We use Equation (13) below to find top heat loss coefficient [1].

$$U_t = \frac{1}{\frac{N_g}{\frac{C}{T_p}\left[\frac{T_p-T_a}{N_g+f}\right]^{0.33}+\frac{1}{H_w}} + \frac{\sigma\left(T_p{}^2-T_a{}^2\right)\left(T_p+T_a\right)}{\frac{1}{\varepsilon_p+0.05N_g\left(1-\varepsilon_p\right)}+\frac{2N_g+f-1}{\varepsilon_g}-N_g}} \tag{13}$$

In the above equation, N_g is the number of glass cover, T_p is the mean absorber temperature, ε_p is the absorber plate emissivity, ε_g is the glass emissivity, h_w is the convection heat transfer coefficient, C is the heat capacity, which will be calculated from Equation (14) below [1].

$$C = 365.9(1 - 0.00883\beta + 0.0001298\beta^2) \tag{14}$$

In this Equation, β is the collector's slope. For obtaining f, following Equation (15) can be used [1].

$$f = (1 - 0.04h_w + 0.0005h_w{}^2)\left(1 + 0.091N_g\right) \tag{15}$$

In Equation (15), we have h_w, which should be found. So, Equation (16) below is used to find it [1]. In this equation, V is the wind velocity, and L is the length of the collector.

$$h_w = \frac{8.6V^{0.6}}{L^{0.4}} \tag{16}$$

The heat escaping from the lower part of the collector is initially transferred through conduction within the insulation and subsequently through a combination of convection and infrared radiation to the surrounding air; thus, the energy loss is given by Equation (17) below [1].

$$U_b = \frac{1}{\frac{t_b}{k_b} + \frac{1}{h_{c,b-a}}} \tag{17}$$

In this Equation (17), t_b is the thickness of back insolation, k_b is the conductivity of back insulation, and $h_{c,b-a}$ is the convection heat loss coefficient from back to ambient. The heat loss from the back of the plate rarely exceeds 10% of the upward loss. Typical values of the back surface heat loss coefficient are 0.3–0.6 W/m^2-K [16]. Similarly, the heat transfer coefficient for the heat loss from the collector edges can be obtained from Equation (18) below.

$$U_e = \frac{1}{\frac{t_e}{k_e} + \frac{1}{h_{c,e-a}}} \tag{18}$$

Next, we can find the absorbed solar radiation S from Equation (19) below [1].

$$S = I_B R_B(\tau\alpha)_B + I_D(\tau\alpha)_D\left[\frac{1+Cos(\beta)}{2}\right] + \rho_G(I_B + I_D)(\tau\alpha)_G\left[\frac{1-Cos(\beta)}{2}\right] \tag{19}$$

$$(\tau\alpha)_{\mathrm{B}} = 1.01\tau\left(\alpha/\alpha_n\right)\alpha_n \tag{20}$$

$$\tau \cong \tau\alpha \tag{21}$$

$$\frac{a}{a_n} = 1 + 2.0345\times10^{-3}\theta_e - 1.99\times10^{-4}\theta_e{}^2 + 5.324\times10^{-6}\theta_e{}^3 - 4.799\times10^{-8}\theta_e{}^4 \tag{22}$$

From Equation (23), the effective incidence angle for diffuse radiation is [1]:

$$\theta_{e,D} = 59.68 - 0.1388\beta + 0.001497\beta^2 \tag{23}$$

To find the declination angle for each month, Equation (24) should be used. In this equation, δ is the declination angle and N is the number of days in the year starting from the 1st of January [1]:

$$\delta = 23.45sin\left[\frac{360}{365}(284 + N)\right] \tag{24}$$

To find the incidence angle for every month throughout the year, Equation (25) is needed. This equation provides the incidence angle of a south-facing tilted collector in the northern hemisphere [1]. In this equation, β represents the surface or collector tilt angle from the horizontal, ω is the hour angle, and L is the latitude.

$$Cos(\theta) = Sin(L-\beta)Sin(\delta) + Cos(L-\beta)Cos(\delta)Cos(h) \quad (25)$$

3. Results and Discussion

The study's findings are summarized in Table 6, which presents the efficiency of both single-glazed and double-glazed collectors at various mass flow rates. The efficiencies are presented for mass flow rates of 0.01 and 0.005 kg/s. Figure 7 shows that the efficiency of the FPC changes very slightly during the year.

Figure 8 shows the efficiencies for both single glaze and double glaze at mass flow rates of 0.01 and 0.005 kg/s. The efficiency variation for single glaze for 0.01 kg/s is very slight, approximately 4.05% over the year, remaining nearly constant at around 0.719. For the mass flow rate of 0.005 kg/s, the efficiency variation is approximately 4.87%, and it remains nearly constant at around 0.619 throughout the year.

The efficiency variation for double glaze for the mass flow rate of 0.01 kg/s is very slight, approximately 2.26% over the year, with a nearly constant value of 0.753. For the mass flow rate of 0.005 kg/s, the efficiency variation is approximately 2.53% over the year, with a nearly constant value of 0.674.

Figure 9 displays the average efficiencies of both single- and double-glazed collectors for a mass flow rate of 0.01 and 0.005 kg/s. It indicates that the percentage difference between efficiency for single glaze and double glaze at a flow rate of 0.01 kg/s is 4.62%. The efficiency variation of single- and double-glazed collectors at a mass flow rate of 0.005 kg/s reveals an 8.51%.

The efficiency of the FPC may not vary significantly with changes in mass flow rate because as the mass flow rate changes, the output temperature also changes. The glaze of the collector affects the efficiency of the FPC because it significantly reduces top heat losses and transmittance.

Table 6
Monthly efficiency of single- and double-glazed collectors for different mass flow rates

	Single glazed		Double glazed	
	0.01 kg/s	0.005 kg/s	0.01 kg/s	0.005 kg/s
January	0.701	0.601	0.742	0.663
February	0.706	0.606	0.745	0.666
March	0.718	0.618	0.753	0.674
April	0.72	0.62	0.754	0.675
May	0.725	0.626	0.757	0.677
June	0.727	0.628	0.758	0.679
July	0.73	0.631	0.759	0.68
August	0.729	0.63	0.759	0.68
September	0.726	0.627	0.758	0.679
October	0.721	0.621	0.755	0.676
November	0.714	0.614	0.75	0.671
December	0.71	0.61	0.747	0.669
Yearly average	0.719	0.619	0.753	0.674
Minimum	0.701	0.601	0.742	0.663
Maximum	0.730	0.631	0.759	0.680

Figure 7
Efficiency of flat-plate collector

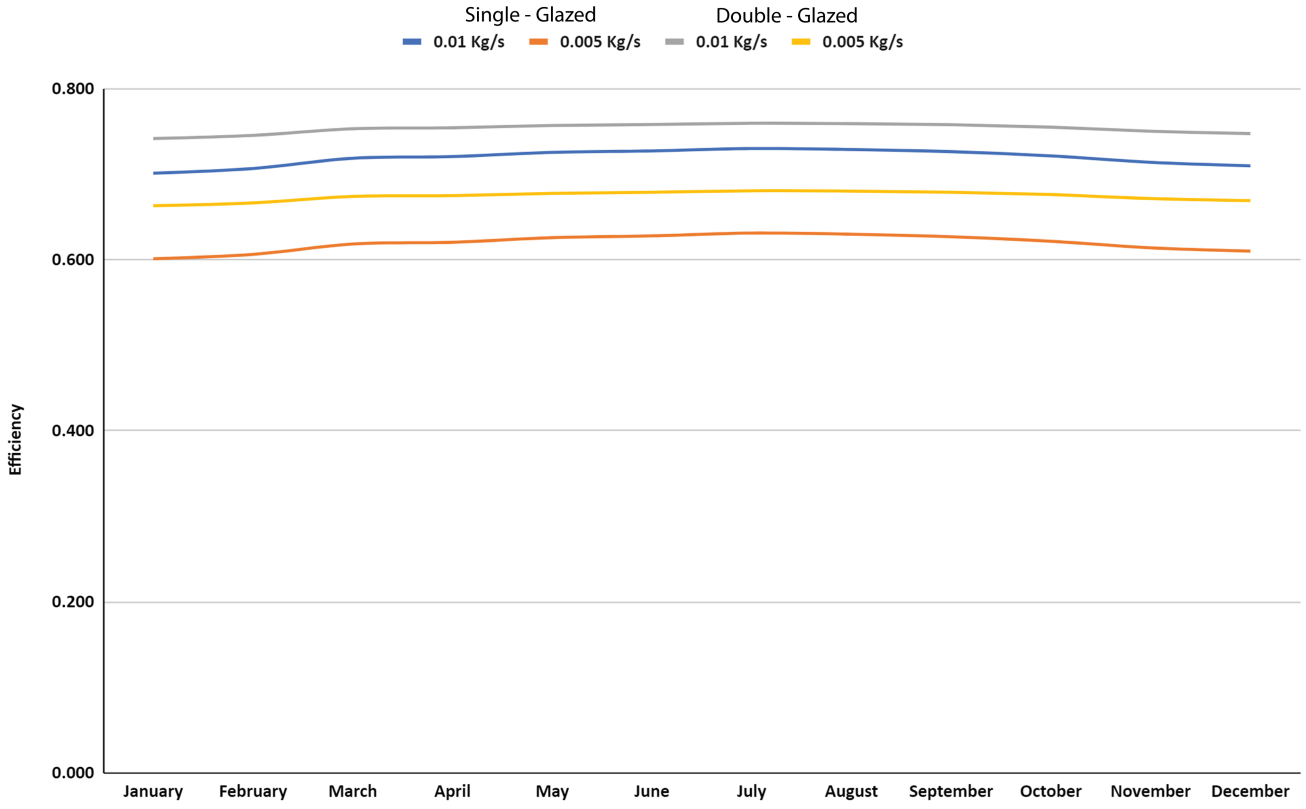

Figure 8
Efficiency compression of single-glazed and double-glazed flat plate collector (FPC) for different mass flow rates

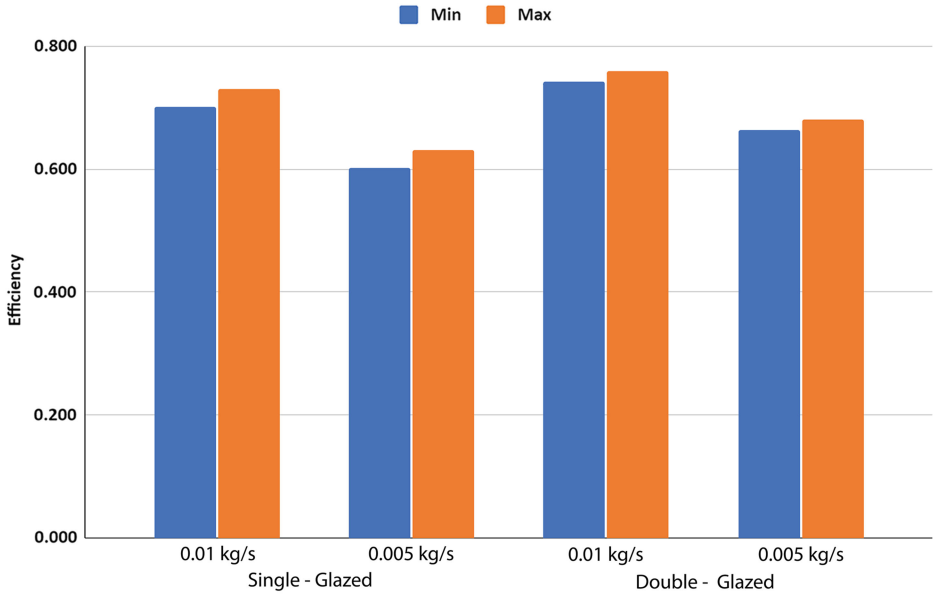

Figure 9
Efficiency of FPC for different glazing at 0.01 and 0.005 kg/s mass flow rate

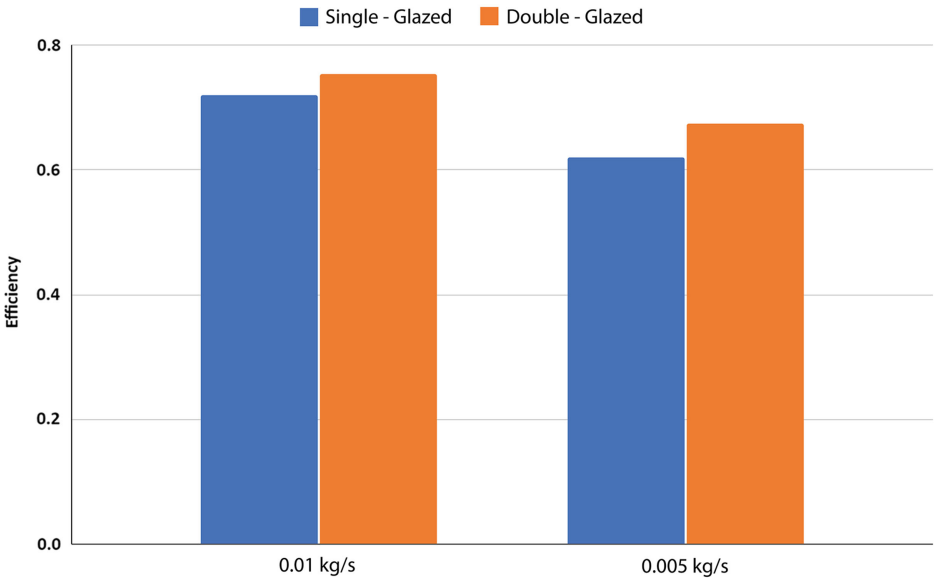

4. Conclusion

In conclusion, this study sheds light on solar water heating systems' substantial benefits and untapped potential, specifically focusing on FPCs. The research underscores the significance of clean and renewable energy sources in addressing our ever-increasing energy demands while minimizing environmental impact. Through meticulous evaluation and comparison of single-glazed and double-glazed collector types, we have demonstrated the tangible efficiency enhancements that can be achieved with thoughtful design. The single-glazed collector, with its commendable efficiency of 0.669, provides a dependable option for harnessing solar thermal energy. However, the greater efficiency exhibited by the double-glazed collector at 0.713 emphasizes the importance of continuous innovation in collector technology. Crucially, this study's findings resonate significantly for regions like Kandahar, where consistent hot water usage, primarily reliant on fossil fuel-based heating, prevails. By transitioning toward solar water heating, societies can substantially reduce carbon emissions, energy costs, and dependence on non-renewable resources.

Moving forward, advancements in solar water heating should prioritize technical efficiency and consider economic viability, local climatic conditions, and user accessibility. Collaborative efforts among researchers, industries, policymakers, and communities will

be pivotal in accelerating the adoption of solar thermal systems. As we stand at a crossroads of energy choices, embracing solar water heating stands out as a progressive stride toward a sustainable future. This study underscores that a clean and prosperous energy landscape is within reach, urging us all to embark on a path of energy-conscious decisions for our planet's benefit and future generations.

Recommendations

The findings state that the FPCs are functioning well and have the potential to play a significant role in the nation's energy landscape. However, for precise calculations of efficiency, further studies and research are required. These studies should be based on accurate data collection and should also analyze the impact of mass flow rate on the output temperature.

Ethical Statement

This study does not contain any studies with human or animal subjects performed by any of the authors.

Conflicts of Interest

The authors declare that they have no conflicts of interest to this work.

Data Availability Statement

Data available on request from the corresponding author upon reasonable request.

Author Contribution Statement

Sayed Ahmad Zamir Fatemi: Conceptualization, Methodology, Software, Validation, Formal analysis, Resources, Data curation, Writing – original draft, Supervision, Project administration. **Wahidullah Zgham:** Methodology, Writing – original draft. **Safiullah Shirzad:** Resources, Writing – review & editing. **Zainullah Serat:** Validation, Data curation, Writing – review & editing.

References

[1] Kalogirou, S. A. (2009). *Solar energy engineering: Processes and systems* (1st ed.), USA: Academic Press.

[2] Candra, O., Chammam, A., Alvarez, J. R. N., Muda, I., & Aybar, H. Ş. (2023). The impact of renewable energy sources on the sustainable development of the economy and greenhouse gas emissions. *Sustainability*, *15*(3), 2104. https://doi.org/10.3390/su15032104

[3] Arif, M. N., Waqas, A., Butt, F. A., Mahmood, M., Khoja, A. H., Ali, M., . . . , & Kalam, M. A. (2022). Techno-economic assessment of solar water heating systems for sustainable tourism in northern Pakistan. *Alexandria Engineering Journal*, *61*(7), 5485–5499. https://doi.org/10.1016/j.aej.2021.11.006

[4] Barone, G., Buonomano, A., Forzano, C., & Palombo, A. (2019). Solar thermal collectors. In F. Calise, M. D. D' Accadia, M. Santarelli, A. Lanzini & D. Ferrero (Eds.), *Solar hydrogen production* (pp. 151–178). Academic Press. https://doi.org/10.1016/B978-0-12-814853-2.00006-0

[5] Kumar, L., Hasanuzzaman, M., Rahim, N. A., & Islam, M. M. (2021). Modeling, simulation and outdoor experimental performance analysis of a solar-assisted process heating system for industrial process heat. *Renewable Energy*, *164*, 656–673. https://doi.org/10.1016/j.renene.2020.09.062

[6] Serat, Z., Fatemi, S. A. Z., & Shirzad, S. (2023). Design and economic analysis of on-grid dolar rooftop PV system using PVsyst software. *Archives of Advanced Engineering Science*, *1*(1), 63–76. https://doi.org/10.47852/bonviewAAES32021177

[7] Ahmed, S. F., Khalid, M., Vaka, M., Walvekar, R., Numan, A., Rasheed, A. K., & Mubarak, N. M. (2021). Recent progress in solar water heaters and solar collectors: A comprehensive review. *Thermal Science and Engineering Progress*, *25*, 100981. https://doi.org/10.1016/j.tsep.2021.100981

[8] Dehghan, M., Pfeiffer, C. F., Rakhshani, E., & Bakhshi-Jafarabadi, R. (2021). A review on techno-economic assessment of solar water heating systems in the Middle East. *Energies*, *14*(16), 4944. https://doi.org/10.3390/en14164944

[9] Gupta, H. K., Agrawal, G. D., & Mathur, J. (2015). Investigations for effect of Al_2O_3–H_2O nanofluid flow rate on the efficiency of direct absorption solar collector. *Case Studies in Thermal Engineering*, *5*, 70–78. https://doi.org/10.1016/j.csite.2015.01.002

[10] Moss, R. W., Shire, G. S. F., Henshall, P., Eames, P. C., Arya, F., & Hyde, T. (2017). Optimal passage size for solar collector microchannel and tube-on-plate absorbers. *Solar Energy*, *153*, 718–731. https://doi.org/10.1016/j.solener.2017.05.030

[11] Zhu, L., Raman, A. P., & Fan, S. (2015). Radiative cooling of solar absorbers using a visibly transparent photonic crystal thermal blackbody. *Proceedings of the National Academy of Sciences, 112*(40), 12282–12287. https://doi.org/10.1073/pnas.1509453112

[12] Lati, M., Mennouche, D., Boughali, S., Bouguettaia, H., & Bechki, D. (2022). Thermal and economical study of a solar collector using natural fibers as thermal insulation. *Energy Sources, Part A: Recovery, Utilization, and Environmental Effects*, *44*(4), 8445–8464. https://doi.org/10.1080/15567036.2022.2121877

[13] Gorjian, S., & Ghobadian, B. (2015). Solar thermal power plants: Progress and prospects in Iran. *Energy Procedia*, *75*, 533–539. https://doi.org/10.1016/j.egypro.2015.07.447

[14] Farhana, K., Kadirgama, K., Noor, M. M., Rahman, M. M., Ramasamy, D., & Mahamude, A. S. F. (2019). CFD modelling of different properties of nanofluids in header and riser tube of flat plate solar collector. *IOP Conference Series: Materials Science and Engineering*, *469*, 012041.

[15] Duraivel, B., Muthuswamy, N., Shaik, S., Cuce, E., Owolabi, A. B., Li, H. X., & Kavgic, M. (2023). Extensive analysis of a reinvigorated solar water heating system using low-density polyethylene glazing. *Energies*, *16*(16), 5902. https://doi.org/10.3390/en16165902

[16] Selvam, S., & Sivarajan, C. (2019). Analysis of solar water heating system. *International Research Journal of Engineering and Technology*, *6*(5), 6248–6252.

[17] Polvongsri, S., & Kiasiroat, T. (2014). Performance analysis of flat-plate solar collector having silver nanofluid as a working fluid. *Heat Transfer Engineering*, *35*(13), 1183–1191. https://doi.org/10.1080/01457632.2013.870003

[18] Global Solar Atlas. (2023). Retrieved from: https://globalsolaratlas.info/map?c=11.523088,8.173828,3

[19] Irshad, A. S., & Noori, A. G. (2022). Evaluating the effects of passive cooling and heating techniques on building energy consumption in Kandahar using CLTD method. *Materials Today: Proceedings*, *57*, 595–602. https://doi.org/10.1016/j.matpr.2022.01.456

[20] Ling, D., Mo, G., Jiao, Q., Wei, J., & Wang, X. (2016). Research on solar heating systems with phase change

thermal energy storage. *Energy Procedia*, *91*, 415–420. https://doi.org/10.1016/j.egypro.2016.06.277

[21] Weather Spark. (2023). *Climate and average weather year round in Kandahār (Afghanistan)*. Retrieved from: https://weatherspark.com/y/106300/Average-Weather-in-Kandah%C4%81r-Afghanistan-Year-Round

[22] Mehrad, A. T. (2021). Assessment of solar energy potential and development in Afghanistan. In *International Conference on Renewable Energy*, *239*, 1–12. https://doi.org/10.1051/e3sconf/202123900012

[23] European Commission. (2023). *Photovoltaic geographical information system*. Retrieved from: https://re.jrc.ec.europa.eu/pvg_tools/en/#MR

[24] Madan, J. V., & Sirse, O. M. (2015). Experimental study on efficiency of solar collector at Nagpur (India) during winter. *International Journal of Scientific & Technology Research*, *4*(8), 231–234.

[25] Jalili Jamshidian, F., Gorjian, S., & Shafiee Far, M. (2018). An overview of solar thermal power generation systems. *Journal of Solar Energy Research*, *3*(4), 301–312.

[26] Cengel, Y. A., & Ghajar, A. J. (2014). *Heat and mass transfer: Fundamentals and applications* (5th ed.). USA: McGraw Hill.

How to Cite: Fatemi, S. A. Z., Zgham, W., Shirzad, S., & Serat, Z. (2025). Feasibility Study of Theoretical Efficiency Calculation for Flat-Plate Collectors in Solar Water Heating Systems. *Archives of Advanced Engineering Science*, *3*(2), 73–82. https://doi.org/10.47852/bonviewAAES32021384